



# A Measurement of the Radiation Environment in the CDF Tracking Volume

R.J. Tesarek <sup>a,\*</sup> S. D'Auria <sup>c</sup> A. Hocker <sup>d</sup> K. Kordas <sup>e</sup>  
S. McGimpsey <sup>a</sup> S. Worm <sup>b</sup>

<sup>a</sup>*Fermilab, Batavia, IL 60510, USA*

<sup>b</sup>*Department of Physics and Astronomy, Rutgers University, Piscataway, NJ  
05549, USA*

<sup>c</sup>*Department of Physics, University of Glasgow, Glasgow G12 800, UK*

<sup>d</sup>*Department of Physics and Astronomy, University of Rochester, Rochester, NY  
14627, USA*

<sup>e</sup>*Department of Physics, University of Toronto, Toronto, Ontario M5S 1A7,  
CANADA*

---

## Abstract

We present direct measurements of the spatial distribution of both ionizing radiation and low energy neutrons ( $E_n < 200$  keV) inside the tracking volume of the collider detector at Fermilab (CDF). Two types of thermal luminescent dosimeters are used for these measurements. Data collected from exposures with different accelerator conditions allow us to separate the radiation fields into contributions from proton beam losses and from proton-antiproton collisions. Using a simple model of a power law in  $1/r$ , where  $r$  is the distance from the beam axis we find the power depends on the distance from the interaction point along the beam axis with the range 1.5–2.0. Predictions based on this model show good qualitative agreement with initial measurements of the leakage currents in the low radius silicon detectors.

*Key words:* Radiation measurement, radiation fields, ionizing radiations, non-ionizing radiations, radiation effects on instruments

*PACS:* 87.66, 04.40.N, 87.53, 87.54, 07.89

---

---

\* Corresponding author.

*Email address:* tesarek@fnal.gov (R.J. Tesarek).

## 1 Introduction

Precision vertex detectors have become a powerful tool in high energy physics for tagging and reconstructing the decays of short lived particles such as beauty and charmed mesons and baryons. The power of these devices arise from their ability to give precise position information at distances of a few centimeters from the interaction region. Unfortunately, these detectors are susceptible to radiation damage which decreases the signal size and increases the overall noise from the detector [1]. With sufficient damage, these devices become effectively non-functional. Because of the high cost of constructing such detectors in capital, manpower and time, it is necessary to estimate the lifetime of the detector so that a replacement can be prepared. A key ingredient in an estimate of the detector lifetime is the type, amount and distribution of the radiation seen by the detector.

Modern studies of the radiation environment use Monte Carlo techniques with extensive computer modeling of the processes producing radiation. All of these studies use as input previous measurements of the radiation damage profiles in a single detector published some time ago [2]. We present here a detailed measurement of the radiation environment seen inside the collider detector at Fermilab (CDF) using thermal luminescent dosimeters (TLDs).

The measurements presented here use Harshaw TLD-700 and TLD-600 types of dosimeters. The TLD-700 dosimeters are made of isotopically pure  ${}^7\text{LiF}$  with trace amounts of Mg and Ti and are sensitive to photons and ionizing radiation. TLD-600 dosimeters are made of isotopically pure  ${}^6\text{LiF}$  with the same trace elements. Sensitivity to neutrons occurs through the reaction  ${}^6\text{Li}(n, \alpha){}^3\text{H}$ .

## 2 Measurement Technique

The radiation field is measured by placing packages of TLD chips at numerous locations in the CDF tracking volume. Each labeled package is made up of a 0.79 mm thick FR-4 holder containing three TLD chips of each type. These chips are held in place with 0.076 mm thick kapton tape. The three chips provide measurement redundancy. To avoid confusing TLDs of different types, each TLD chip type is a different shape. The round TLD-700 chips measured 4.2 mm in diameter by 0.9 mm thick. The square TLD-600 chips measured  $3.4 \times 3.4 \times 0.9 \text{ mm}^3$ . Figure 1 shows the physical layout of a TLD package.

TLD packages are installed in three regions in the tracking volume. For the first region, packages are placed on the inner faces of the CDF endplug calorime-

ters,  $\pm 175$  cm from the interaction point, at 8 locations in azimuth ( $\phi$ ) and 5 locations in radius ( $r$ ) from the detector axis (80 locations). For the second region, packages are installed on the outside of the carbon fiber support structure for the inner silicon (SVX,  $r=17.7$  cm) at 5 locations along the detector axis ( $z$ ) and at 5 locations in azimuth (25 locations). The third region has packages installed on the carbon fiber support structure for the intermediate silicon (ISL,  $r=37.7$  cm) at 5 locations along the detector axis and 8 azimuthal locations (40 locations). The  $z$  and  $\phi$  locations for the ISL packages are the same as those for the SVX packages. Additional packages were made and set aside to provide a control dose. A total of 916 dosimeters are used in these measurements.

Installing and harvesting the packages in regions 2 and 3 is accomplished using kapton tape to affix each package to a Mylar leader approximately 6 m long. The ends of the kapton tape are then glued to help keep the tape attached to the leader and smooth the transition between bare leader and leader + tape. This leader is then pulled through eyelets at fixed locations on the carbon fiber support structures. By taping a new leader to the end of an old leader, we install new packages of dosimeters at the same time we harvest old packages.

### 3 Calibration and Dosimetry

The TLD response to photons is measured by exposing each TLD chip to a known dose from a well calibrated source and measuring the light yield as the chip is heated. These calibrations are performed at Fermilab's Radiation Physics Calibration Facility using a 1 Rad exposure to a  $^{137}\text{Cs}$  source [4]. The neutron response for the TLD-600s is calibrated with a 10 mrad exposure to  $^{252}\text{Cf}$  which undergoes radioactive decay via spontaneous fission. Approximately 20 neutrons are liberated in the decay with a neutron energy peaking at approximately 2 MeV [3]. The light yield measurements from each chip is made by the Fermilab radiation safety group using a Harshaw model 2000 TLD reader [5]. The TLD reader records the total charge in nC integrated from a PMT viewing the TLD chip during heating. We find the chip-to-chip variation in photon response to be 2.7% and 3.2% for the TLD-700 and TLD-600 dosimeters, respectively. The photon response of individual TLD chips was found to be reproducible to less than 1%. The chip-to-chip variation in neutron response was measured to be 15% .

The TLDs used for these measurements are known to exhibit superlinearity for doses above 100 rad; ie, more light is emitted than predicted by a linear model. In order to characterize this non-linearity, we measure the response of a sample of 10 TLD-700 and 10 TLD-600 chips to known photon doses in the range 1–10,000 rad. The ionizing radiation dose is calculated using the

TLD response to a 1 rad exposure and correcting for the non-linearity in TLD response and subtracting the control dose. The neutron dose is calculated by first calculating the normalized response, correcting for non-linearity and subtracting the photon dose from the TLD-700 data. Typical control doses are 1-10 mrad.

## 4 Measurements

Dosimeters are installed and replaced only during significant periods of accelerator down time. For the data reported here, we include two exposures; February 23 – May 1 and May 1 – October 8 of 2001. Beam conditions during these exposures are recorded using multiple devices. The number of collisions (accelerator luminosity) is measured at CDF using a new device which detects the Cherenkov radiation from charged particles originating from the interaction region [6]. Losses from the proton and antiproton beam are measured using a two sets of scintillation counters surrounding the beam pipe and located on either side of the CDF detector. Proton losses are calculated as the coincidence of the counter signals with the timing of protons as they pass the plane of the counters on their way into the CDF interaction region. Similar measurements are made for antiproton losses. Table 1 summarizes the exposure statistics for the two periods above. From the table, we see that proton losses the first period while proton-antiproton collisions dominate the second period.

Figure 2 shows the ionizing and neutron radiation doses for the two exposure periods as a function of the coordinate along the beam line ( $z$ ). The curves on each plot are to connect the data from measurements taken at different radii from the detector axis. The proton beam travels in the  $+z$  direction. Each point on the plot is the average over the  $\phi$  measurements at that  $z$  position with uncertainties calculated as the RMS spread of the measurements. Note the different pattern in the  $z$  direction in the ionizing radiation for the two periods. The pattern for the collision dominated period is roughly symmetric about the  $z = 0$  while the pattern for the loss dominated period is asymmetric in  $z$ . The later pattern is consistent with lost protons and secondaries from beam gas events being restricted by a small aperture on the  $-z$  side of the detector. Antiprotons are expected to produce a similar pattern, but the effect is reduced by the antiproton to proton ratio in the two beams of 1:10.

To obtain radiation patterns associated with losses and collisions, one may assume that the overall radiation environment is a linear super-position of the two contributions. For the two periods listed above, this gives two equations and two unknown distributions. Solving for the the two patterns yields the result in Figure 3. The shaded band in the figure represents the systematic

uncertainty on the loss measurement. Normal accelerator running conditions are closer to those from the second period where the ratio of losses/collisions is  $3.9 \times 10^9$  loss counts/pb<sup>-1</sup>.

## 5 Modeling

In order to predict the radiation seen by various detector components, one needs a model to extrapolate the above measurements to device locations. We use a model based on previous experience from silicon damage profiles measured in the CDF detector [2]. This model assumes that the radiation field surrounding the interaction region is cylindrically symmetric and follows a power law in  $1/r$ , where  $r$  is the distance from the beam axis. We fit the data at each  $z$  location to the functional form:

$$D = \frac{A}{\{(x - x_0)^2 + (y - y_0)^2\}^{\frac{\alpha}{2}}}, \quad (1)$$

where  $A$  is an absolute normalization,  $\alpha$  is the power law and  $(x_0, y_0)$  is the beam-detector relative offset. The normalization and power law results are summarized in Figure 4 as a function of  $z$ .

The radiation field predicted by these measurements can be tested by comparing particle fluxes calculated from leakage current measurements in the low radius silicon detectors. The particle flux is calculated by measuring the slope in the silicon leakage current as a function of accelerator delivered luminosity. The rate of increase in the current is corrected from 8° C to 20° C and a damage factor of  $3.0 \times 10^{-17}$  A/cm. The dose rate in the TLDs is converted to a particle flux using the conversion factor of  $3.87 \times 10^7$  minimum ionizing particles (MIP)/rad and dividing the result by  $10.7$  pb<sup>-1</sup>. Figure 5 compares the particle flux from leakage current data for the innermost layer of silicon ( $r = 1.7$  cm) with the prediction from the TLD data. The fractional deviation between the two is approximately 25%.

## 6 Summary

We use thermal luminescent dosimeters to measure the spatial distribution of the radiation field inside the CDF tracking volume. These measurements include the components due to ionizing radiation and low energy neutrons ( $E_n < 200$  keV). We find different radiation patterns for proton beam losses and for proton-antiproton collisions and have separated the total field into

these two components. A simple model based on previous experience is consistent with the data to within 20%. Extrapolation of the TLD data agrees within 25% with the particle flux calculated from silicon leakage currents.

## References

- [1] C. Leroy, S. Bates, B. Dezillie, M. Glaser, F. Lemeilleur and I. Trigger, Nucl. Instr. Meth. **A388**, (289) 1997; F. Lemeilleur, M. Glaser, E. H. Heijne, P. Jarron and E. Occelli, IEEE Trans. Nucl. Sci. **39**, (551) 1992;
- [2] D. Amidei, *et al.* Nucl. Instr. and Meth. **A350** (73) 1994.
- [3] National Nuclear Data Center, Brookhaven National Laboratory, Upton, NY 11973-5000 (<http://www.nndc.bnl.gov>).
- [4] F. Krueger, S. Hawke, "Calibration and On-Axis Characterization of the Source Projector Facility at the Radiation Physics Calibration Facility", Fermilab Radiation Physics internal note **121**, January 1996.
- [5] Harshaw model 2000 TLD reader: Thermo RMP, 6801 Cochran Road, Solon, OH 44139, USA. The model 2000 TLD reader used for these measurements was modified to extend the reading cycle to 1 second.
- [6] J. Elias, *et al.* Nucl. Instr. and Meth. **A441** (366-373), 2000. D. Acosta, *et al.* Nucl. Instr. and Meth. **A461** (540-544), 2001.

Table 1

Summary of beam conditions at CDF for the two exposure periods in 2001.

Period	Beam ( $\times 10^{19}$ )		Losses ( $\times 10^9$ )		$\int \mathcal{L} dt$ ( $\text{pb}^{-1}$ )
	P	$\bar{P}$	P	$\bar{P}$	
Feb. – May 2001	0.0703	0.0082	15.3	2.02	0.058
May – Oct. 2001	1.56	0.137	40.9	10.2	10.7

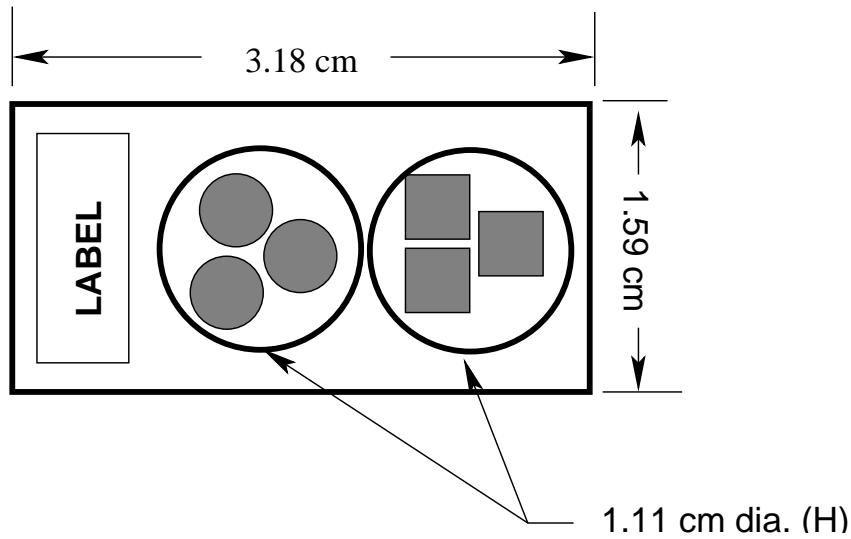


Fig. 1. TLD package made from 0.79 mm thick FR-4 showing TLD-700 (round) and TLD-600 (square) dosimeters. The holes are covered with 76  $\mu\text{m}$  thick kapton tape.

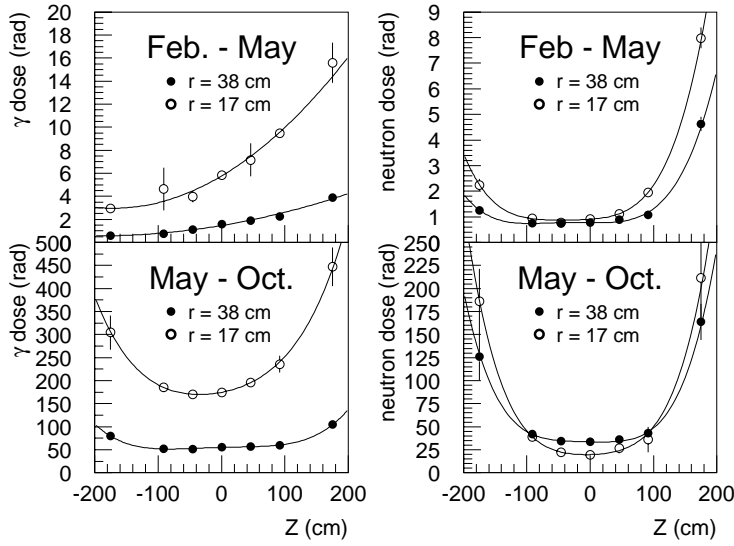


Fig. 2. Ionizing (left plots) and low energy neutron (right plots) radiation dose as a function of  $z$ ; protons travel in the  $+z$  direction. The top and bottom plots are for the two exposure periods. Curves on the plots serve only to guide the eye.

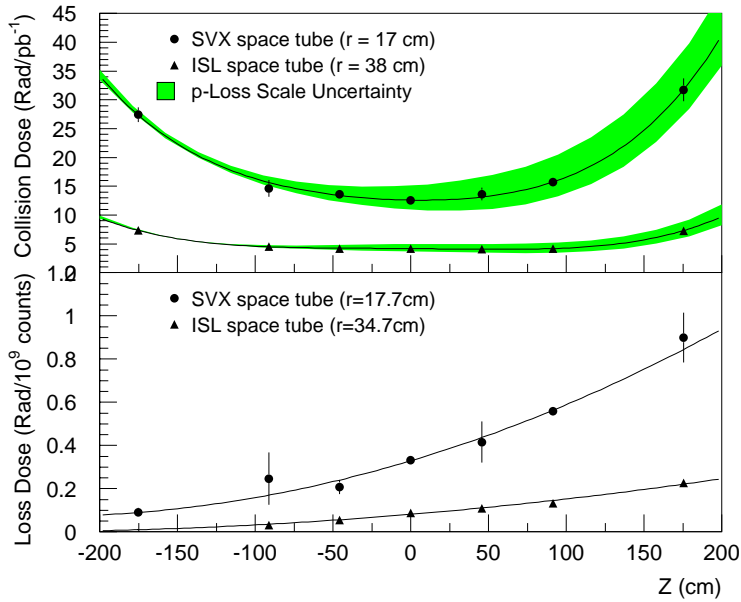


Fig. 3. Ionizing radiation separated into components due to collisions (top) and proton beam losses (bottom).

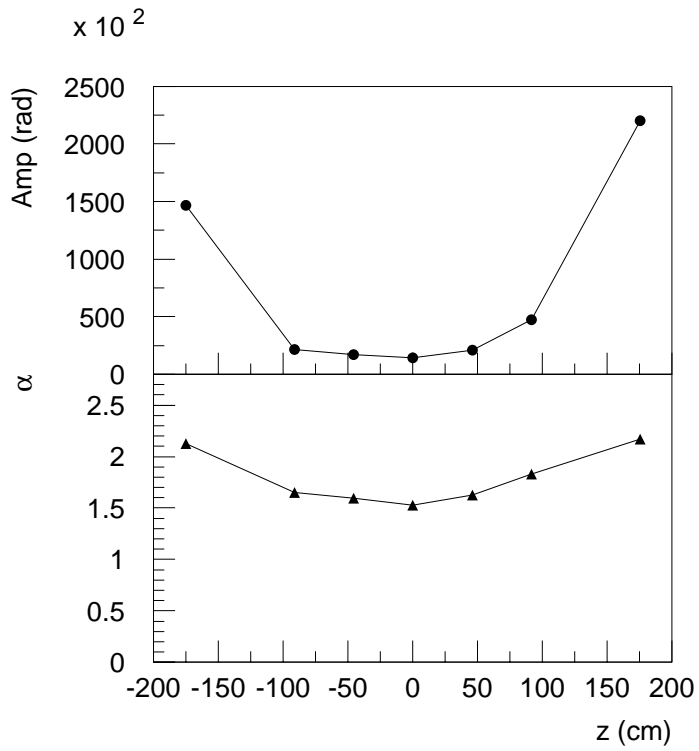


Fig. 4. Normalization,  $A$  (top) and power law exponent,  $\alpha$  (bottom) from the model described in the text as a function of  $z$ . The results are shown only for the May – Oct. 2001 exposure.

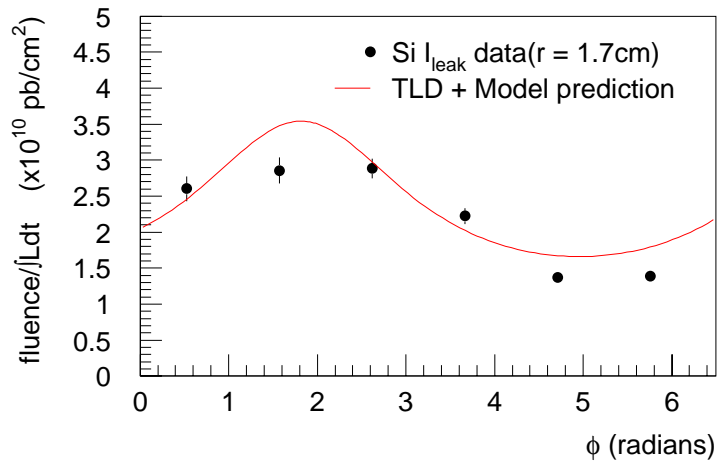


Fig. 5. Charged particle fluence rate as a function of  $\phi$  for the innermost layers of silicon (L00). The points are calculations from leakage current data. The curve is a prediction based on TLD measurements.